SPANDIDOS PUBLICATIONS

INTERNATIONAL JOURNAL OF MOLECULAR MEDICINE 46: 1146-1154, 2020

hsa_circ_0058092 protects against hyperglycemia-induced endothelial progenitor cell damage via miR-217/FOXO3

JIE CHENG[1,2*], WEIWEI HU[3*], FENGHUI ZHENG[4*], YONGFA WU[1,2] and MAOQUAN LI[1,2]

[1]Department of Interventional and Vascular Surgery, Tenth People's Hospital of Tongji University; [2]Institute of Interventional and Vascular Surgery, Tongji University; [3]Institute of Tropical Medicine, Guangzhou University of Traditional Chinese Medicine, Guangzhou, Guangdong 510405; [4]Department of Endocrinology and Metabolism, Tenth People's Hospital of Tongji University, Shanghai 200072, P.R. China

Received March 5, 2020; Accepted June 4, 2020

DOI: 10.3892/ijmm.2020.4664

Abstract. Circular RNAs (circRNAs) regulate the expression of genes that are critical for various biological and pathological processes. Previous studies have reported that the expression of hsa_circ_0058092 is decreased in patients with diabetes mellitus (DM); however, the specific role of this circRNA in DM is unknown. In the present study, endothelial progenitor cells (EPCs) were isolated and a decreased hsa_circ_0058092 expression was found under conditions of hyperglycemia (HG). The overexpression of hsa_circ_0058092 protected the EPCs against HG-induced damage by preserving cell survival, proliferation, migration and angiogenic differentiation. The overexpression of hsa_circ_0058092 also decreased the HG-induced increase in NADPH-oxidase proteins and inflammatory cytokines. Further investigation revealed that the overexpression of hsa_circ_0058092 enhanced FOXO3 expression, which was mediated through the interaction with miR-217. Furthermore, the upregulation of miR-217 or the downregulation of FOXO3 abolished the protective effects of hsa_circ_0058092 against HG-induced EPC damage. On the whole, these data suggest that hsa_circ_0058092 acts via the miR-217/FOXO3 pathway to protect against EPCs HG-induced damage, and to preserve the migration and angiogenesis of EPCs.

Correspondence to: Dr Yongfa Wu or Dr Maoquan Li, Department of Interventional and Vascular Surgery, Tenth People's Hospital of Tongji University, 301 Middle Yan Chang Road, Guangzhou, Guangdong 510405, P.R. China
E-mail: slkyongfa@126.com
E-mail: cjr.limaoquan@vip.163.com

[*]Contributed equally

Abbreviations: circRNAs, circular RNAs; miR-217, microRNA-217; miRNAs, microRNAs; EPCs, endothelial progenitor cells; FOXO3, forkhead box O 3; ROS, reactive oxygen species

Key words: hsa_circ_0058092, miR-217, FOXO3, endothelial progenitor cells, high glucose, diabetes mellitus

Introduction

Impaired wound healing is a major complication of diabetes mellitus (DM) and despite the associated risks, treatment strategies for diabetic-related wounds are limited. Endothelial dysfunction is an indicator of diabetes-induced macrovascular complications (1,2). Vascular differentiation at injury sites affects the speed of wound healing, while the homing and angiogenic differentiation of endothelial progenitor cells (EPCs) are critical for successful wound healing (3). EPCs are immature endothelial cells that can proliferate and differentiate to promote new blood vessel formation at injury sites. EPCs can also secrete various angiogenic and vasoactive factors to enhance angiogenesis (4-6). Endothelial dysfunction is closely related to the occurrence and development of vascular disease and is also an intrinsic cause of impaired wound healing (7). It has been suggested that the dysregulation of EPC phenotypes and functions in patients with DM may be attributed to the aberrant signaling of cytokines and other molecules. Indeed, it has been reported that high glucose levels promote EPC dysfunction and induce EPC apoptosis (8). Through inflammatory responses and the NADPH oxidase (NOX)-mediated overproduction of reactive oxygen species (ROS), hyperglycemia (HG) alone can induce alterations in gene expression and cellular behaviors in DM (9,10). However, the specific mechanisms of HG-induced endothelial cell injury are unclear.

CircRNAs are closed circular RNA molecules that function as competitive endogenous RNAs by regulating transcription and blocking the miRNA-mediated inhibition of target genes (11). CircRNAs are implicated in a number of diseases and their differential expression plays a crucial role in disease development processes (12). It has been reported that circRNAs participate in the regulation of insulin secretion and diabetes pathogenesis (13). The expression of circRNA hsa_circ0054633 and circRNA Cdr1 in peripheral blood can be used as a diagnostic biomarker for both type 2 DM (T2DM) and pre-diabetes (14,15). The expression of circRNA circANKRD36 has been shown to be upregulated in peripheral blood leukocytes, and this increased expression is associated with chronic inflammation in T2DM (16). It has been reported that the expression of hsa_circ_0058092 is downregulated

in patients with DM (17); however, the role of this circRNA in HG-induced EPC damage remains unclear. Thus, using *in vitro* approaches, the present study aimed to identify the mechanisms through which the decreased expression of hsa_circ_0058092 induces EPC damage under HG conditions.

Materials and methods

EPC characterization and isolation. Peripheral blood from healthy volunteers was diluted twice in phosphate-buffered saline (PBS) and the solution was gently layered over 4 ml of lymphocyte separation liquid (Sigma-Aldrich; Merck KGaA). The present study was approved by the Ethics Committee of the Tenth People's Hospital of Tongji University after obtaining informed patient consent (SHDSYY-2019-3322). The tubes were centrifuged at 800 x g for 30 min at 4˚C. Peripheral blood mononuclear cells (PBMCs) at the interface were then transferred to a new tube and washed with PBS by centrifugation at 400 x g for 5 min at 4˚C. EPCs were cultured from PBMCs in 24-well plates ($5x10^6$ cells/well) in endothelial cell basal medium-2 (Lonza Group, Ltd.). The cells were cultured continuously for 10 days and then utilized for co-culture experiments. Subsequently, $CD133^+$ EPCs were selected using CD133-coupled magnetic microbeads (Miltenyi Biotech) according to standard processing procedures. Following isolation, $CD133^+$ EPCs were expanded in endothelial cell basal medium-2 as previously described (17).

To analyze CD14, CD45, kinase insert domain receptor (KDR) and CD34 expression, the EPCs were incubated at 4˚C with a biotinylated anti-rat IgG (H1L) horse antibody (1:200) (cat. no. AI-2001, Vector Laboratories) for 12 h and (1:200) FITC-conjugated streptavidin (cat. no. 9013-20-1, Caltag Laboratories) for 1 h. Following treatment, the EPCs were fixed in 1% paraformaldehyde. Quantitative analyses were performed using FlowJo software (FlowJo, LLC) and a FACSCalibur flow cytometer.

Reagent generation and cell treatment. FOXO3 overexpression vector (using pcDNA3.1 vector), miR-217 mimic/inhibitor and hsa_circ_0058092 overexpression vector (using pcDNA3.1 vector) were generated by GenePharm Co. Ltd. The EPCs were maintained at approximately 40% confluence and cells were transfected with the different vectors (50 ng) using Lipofectamine 2000 (Invitrogen; Thermo Fisher Scientific, Inc.) for 48 h before treatment with high glucose (30 mM). An Empty pcDNA3.1 vector was used as the control for FOXO3 and hsa_circ_0058092 overexpression. The negative controls for miR-217 mimic/inhibitor (50 ng) (were provided by GenePharm Co. Ltd.) were also transfected into EPCs using Lipofectamine 2000 for 48 h prior to treatment with high glucose (30 mM).

In vitro tube formation assay. *In vitro* Matrigel tube formation assays were performed to determine the angiogenic activity of EPCs (18). Briefly, the EPCs ($5x10^4$ cells) transfected with or without hsa_circ_0058092 overexpression vector or siFOXO3 vector were seeded in Matrigel-coated 48-well plates with or without HG treatment for 12 h. After this period, tubular EPC structures were examined under a microscope (Axioplan 2 imaging E, Carl Zeiss). The total number of tubes, which served as a measure of *in vitro* angiogenesis, were scanned and quantified from 3 random fields of view in each well at x100 magnification.

Cell proliferation assay. The cell counting kit-8 (CCK-8; Invitrogen; Thermo Fisher Scientific, Inc.) was used to assess EPC proliferation following standard protocols. Briefly, $2x10^4$ EPCs were seeded in 100 μl of DMEM in 96-well plates. Cell viability was measured 0, 24, 48 and 72 h after seeding by the addition of 10 μl of CCK-8 solution to the wells using Thermo Scientific Microplate Reader (Thermo Fisher Scientific, Inc.).

Western blot analysis. Protein was extracted from the EPCs using RIPA lysis buffer (Sigma-Aldrich; Merck KGaA). Protein concentrations were quantified using the BCA Protein Assay kit (Vigorous Biotechnology Beijing Co. Ltd.). Proteins were then resolved by sodium dodecyl sulfate polyacrylamide gel electrophoresis (SDS-PAGE, 12% concentrated adhesive and 4% separated adhesive) and transferred to nitrocellulose membranes (EMD Millipore). The membranes were blocked in non-fat milk (5%) before being incubated with the primary antibodies NOX1 (1:200, cat. no. sc-130543, Santa Cruz Biotechnology, Inc.) and NOX4 (1:200, cat. no. sc-518092, Santa Cruz Biotechnology, Inc.) at 4˚C for 12 h and horseradish peroxidase-coupled secondary antibodies IgG (1:200, cat. no. sc-516102, Santa Cruz Biotechnology, Inc.) at 4˚C for 4 h. Glyceraldehyde 3-phosphate dehydrogenase (GAPDH) (1:200, cat. no. sc-365062, Santa Cruz Biotechnology, Inc.) was used as an internal control and detected using an ECL detection kit (cat. no. SL100309, SignaGen).

RNA extraction and RT-qPCR. RNA extractions were performed using TRIzol reagent (Invitrogen; Thermo Fisher Scientific, Inc.) according to a previously described protocol (19). The pTRUEscript First Strand cDNA Synthesis kit (Aidlab) was used for cDNA synthesis with 2X SYBR-Green qPCR mix. cDNA was used for RT-qPCR detection and reactions were conducted on an ABI 7900HT sequence detection system (Thermo Fisher Scientific, Inc.). Data were processed using the $2^{-\Delta\Delta Cq}$ method (20). The primers utilized to for PCR were as follows: *hsa_circ_0058092* expression forward, 5'-GAATAA TCAGAAGAGCGAGCC-3' and reverse, 5'-GTCTGGACC AATGTTGGTGAATCG-3'; *miR-217* forward, 5'-CGCAGA TACTGCATCAGGAA-3' and reverse, 5'-CTGAAGGCA ATGCATTAGGAACT-3'; *FOXO3* forward, 5'-GCGTGCCCT ACTTCAAGGATAAG-3' and reverse, 5'-GACCCGCATGAA TCGACTATG-3'; *U6* forward, 5'-CTCGCTTCGGCAGCA CA-3' and reverse, 5'-AACGCTTCACGAATTTGCGT-3'; and *GAPDH* forward, 5'-GCACCGTCAAGGCTGAGAAC-3' and reverse, 5'-GGATCTCGCTCCTGGAAGATG-3'.

Migration assay. For cell migration analysis, the EPCs were placed into a Transwell upper chamber (8-μm pore membrane, BD Biosciences) at a density of $1x10^5$ cells in 200 μl of serum-free medium. Complete EPC medium (500 μl) was added to the bottom chamber. Following 1 day of culture (at 37˚C in a humidified atmosphere with 5% CO_2), the EPCs in the bottom chamber were fixed in 4% paraformaldehyde, stained with 0.1% crystal violet (cat. no. C8470-5, Beijing Solaibao Technology Co. Ltd.) at room temperature for 20 min,

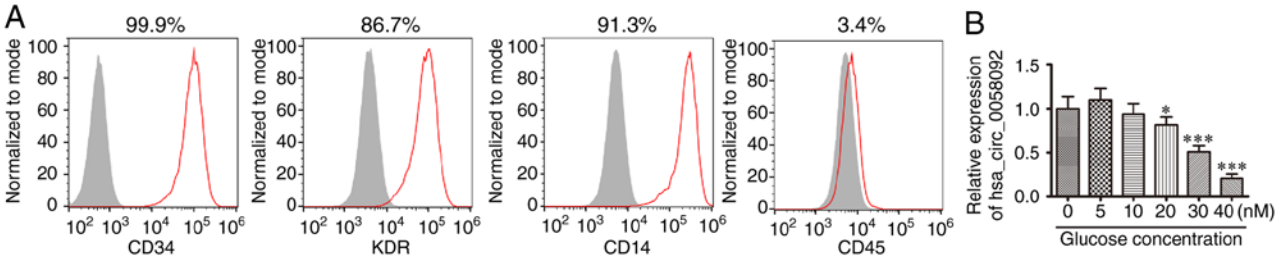

Figure 1. HG decreases the expression of hsa_circ_0058092 in EPCs. (A) Flow cytometric analysis of cell surface markers in human peripheral blood-derived EPCs (CD34, KDR, CD45 and CD14). (B) RT-qPCR detection for the expression of hsa_circ_0058092 in EPCs following treatment with various glucose concentrations (0-40 mM). Data are presented as the means ± SD. *P<0.05, ***P<0.001 vs. control. EPCs, endothelial progenitor cells.

and counted using a microscope (Axioplan 2 imaging E, Carl Zeiss).

Bioinformatics analyses. The Circular RNA Interactome websites for circRNA and miRNA (https://circinteractome.nia.nih.gov/) were used to predict interactions. The target sites between miR-217 and FOXO3 3'UTR were predicted using the TargetScan web-based tool (http://www.targetscan.org/vert_71/).

Enzyme-linked immunosorbent assay (ELISA) for the determination of the levels of soluble inflammatory cytokines. Cytokine interleukin (IL)-6, tumor necrosis factor (TNF)-α and IL-1β concentrations were quantified in the supernatants from EPC cultures using commercially available ELISA kits (Shanghai Senxiong Technology Industry Co., Ltd.). Supernatants were stored at -80˚C prior to analysis following standard procedures. Standards and samples were assayed in triplicate. The $OD_{450\ nm}$ was calculated by subtracting background readings and plotting standard curves using a Thermo Scientific Microplate Reader (Thermo Fisher Scientific, Inc.).

Flow cytometry. Flow cytometry was used to define the EPC apoptotic rates. The integrative application of propidium iodide (PI) and Annexin V (AV)-FITC (cat. no. 40302ES20, Yeasen) was used to differentiate the viable cells from apoptotic or necrotic cells. The cells were washed twice and adjusted to a concentration of $1x10^6$ cells/ml in cold D-Hank's buffer. PI (10 μl) and AV-FITC (10 μl) were added to 100 μl of cell suspension and incubated for 15 min at room temperature in the dark. Finally, 400 μl of the binding buffer were added to each sample without washing, and then analyzed by flow cytometry (D2060R, ACEA NovoCyte, Agilent Technologies, Inc.). The experiments were performed at least 3 times.

Dual luciferase reporter assay. Reporter plasmids were generated by inserting the FOXO3 3'UTR sequence or circRNA into the pGL3 plasmid (Promega Corp.). Reporter plasmids and miR-217 mimics were co-transfected into 293T cells (from the Cell Bank of the Chinese Academy of Sciences, Shanghai) using Lipofectamine 2000. Following culture at 37˚C in a humidified atmosphere with 5% CO_2 for 2 days, Firefly and *Renilla* luciferase activities were detected using the Dual Luciferase Reporter Assay System (Promega Corp.) following standard procedures.

Statistical analysis. Data are expressed as the means ± standard deviation (SD). GraphPad Prism software, version 5.0 (GraphPad, Inc.) was used to compare differences between groups. The differences between groups were assessed using one-way variance analysis with Tukey's post hoc test (compared with all pairs of columns). P-values ≤0.05 was considered to indicate a statistically significant difference.

Results

Overexpression of hsa_circ_0058092 reverses HG-induced EPC damage. Human peripheral blood-derived EPCs were isolated to characterize the role of hsa_circ_0058092 in HG-induced vascular endothelial cell injury. These EPCs were positive for expression of CD14, KDR and CD34, but not for the expression of the leukocyte marker, CD45 (Fig. 1A). These observations suggested that the isolated cells were indeed EPCs, as previously demonstrated (21). The EPCs were then incubated in 0-40 mM glucose for 24 h. RT-qPCR quantification verified that hsa_circ_0058092 expression decreased with the increasing glucose concentrations (Fig. 1B) and 30 mM glucose was selected as the concentration for HG used in subsequent experiments.

To ascertain whether hsa_circ_0058092 plays a protective role in EPCs under HG conditions, a hsa_circ_0058092 overexpression plasmid was constructed and transfected into EPCs. The expression of hsa_circ_0058092 increased significantly at 48 h following transfection with the overexpression plasmid (Fig. 2A). The results of CCK-8 assay revealed that HG conditions suppressed the proliferation of the EPCs, while the overexpression of hsa_circ_0058092 partially restored the proliferative capacity of the EPCs under HG conditions (Fig. 2B). Western blot analysis revealed that HG conditions increased the expression of the oxidative stress-related proteins, NOX1 and NOX4; however, the overexpression of hsa_circ_0058092 suppressed the expression of both these proteins (Fig. 2C). This observation suggested that hsa_circ_0058092 regulated HG-induced oxidative stress. The EPC apoptotic rates were determined using Annexin V/PI staining at 1 day following exposure to HG. The data indicated that the overexpression of hsa_circ_0058092 suppressed the HG-induced apoptosis of EPCs (Fig. 2D and E).

Transwell migration experiments revealed that EPC migration was inhibited under HG conditions; however, migration was restored by the overexpression of hsa_circ_0058092 (Fig. 2F and G). The capacity of EPCs to form tubes was also

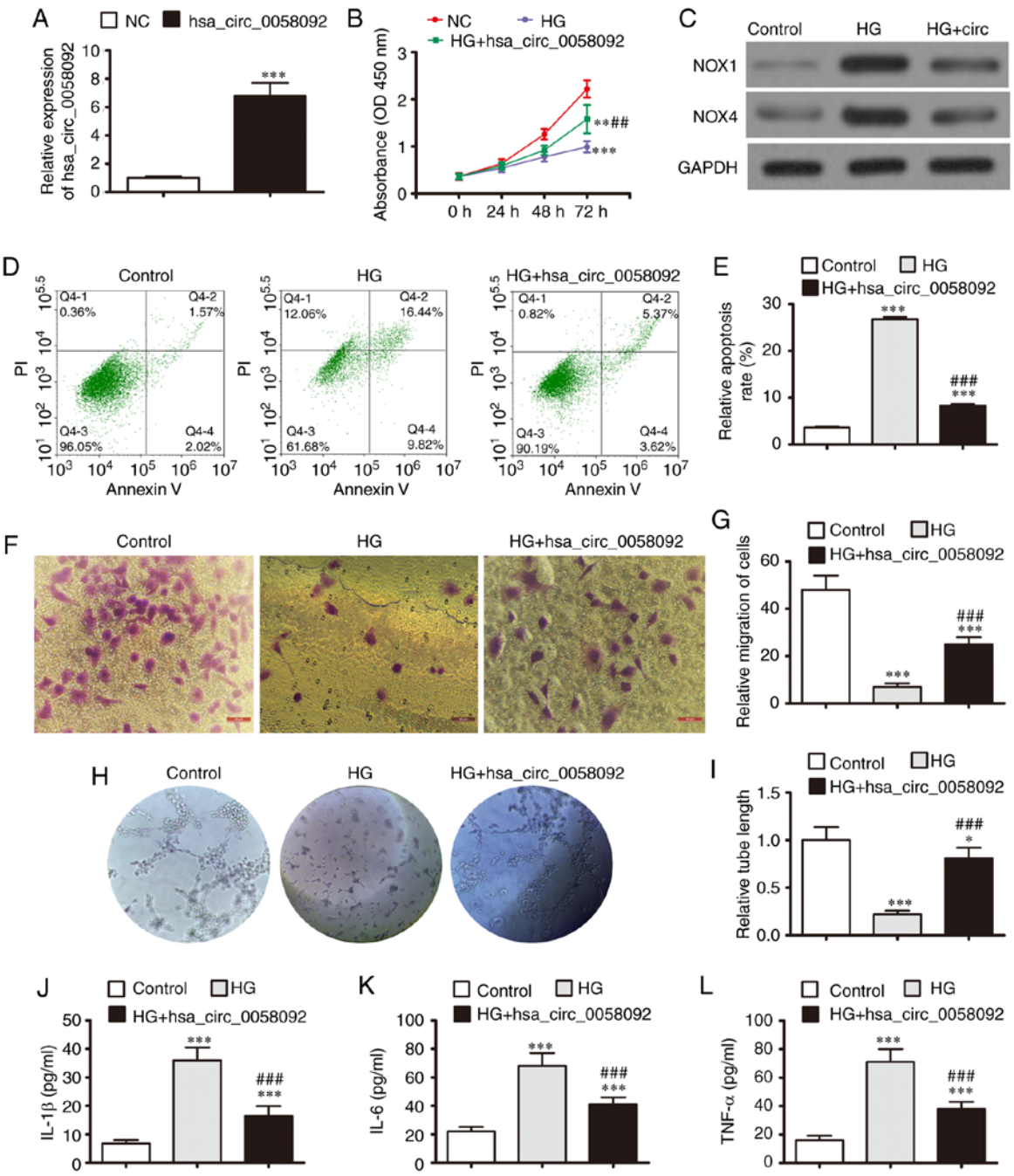

Figure 2. Overexpression of hsa_circ_0058092 reverses EPC damage induced by 30 mM glucose (HG). (A) RT-qPCR detection for the expression of hsa_circ_0058092 in EPCs following transfection with hsa_circ_0058092 overexpression vector. Data are presented as the means ± SD. ***P<0.001 vs. normal control (NC). (B) CCK-8 assay for the proliferation of EPCs. Data are presented as the means ± SD. **P<0.01, ***P<0.001 vs. NC; $^{\#\#}$P<0.01 vs. HG. (C) Expression of the oxidative stress proteins, NOX1 and NOX4, measured by western blot analysis. GAPDH served as an internal control. (D and E) Apoptosis of EPCs determined by Annexin V/PI staining 24 h following HG induction. Data are presented as the means ± SD. ***P<0.001 vs. NC; $^{\#\#\#}$P<0.001 vs. HG. (F and G) Transwell assays for the migration of EPCs. Data are presented as the means ± SD. ***P<0.001 vs. NC; $^{\#\#\#}$P<0.001 vs. HG. Scale bar, 95 μm. (H and I) EPC tube formation capabilities were measured (magnification, 200). Data are presented as the means ± SD. *P<0.05, ***P<0.001 vs. NC; $^{\#\#\#}$P<0.001 vs. HG. (J-L) Levels of the inflammatory cytokines, IL-1β, IL-6 and TNF-α, were measured by ELISA. Data are presented as the means ± SD. ***P<0.001 vs. NC; $^{\#\#\#}$P<0.001 vs. HG. EPCs, endothelial progenitor cells; HG, high glucose.

analyzed. Tube formation was decreased under HG conditions and was restored by the overexpression of hsa_circ_0058092 (Fig. 2H and I). The levels of the inflammatory cytokines, IL-6, TNF-α and IL-1β, were then measured by ELISA. The results revealed that the HG-induced expression of inflammatory cytokines was suppressed by the overexpression of hsa_circ_0058092 (Fig. 2J-L). In summary, these results demonstrated that the overexpression of hsa_circ_0058092 promoted EPC survival, proliferation, migration and tube formation under HG conditions. However, the specific regulatory mechanisms underlying these effects need to be determined.

miR-217 is a target of hsa_circ_0058092. Increasing evidence has indicated that circRNAs regulate gene expression by targeting miRNAs (22). In the present study,

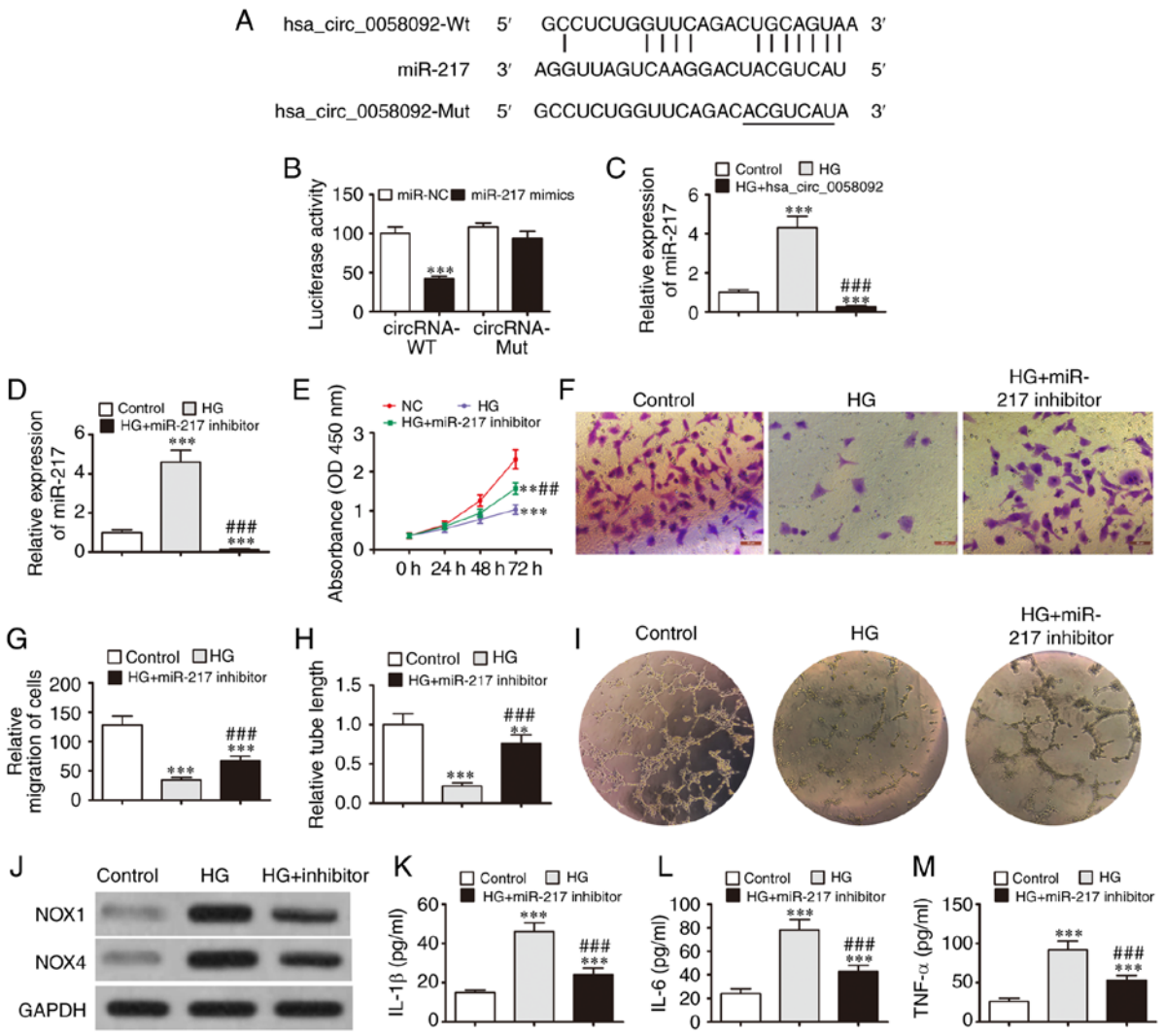

Figure 3. miR-217 is a target of hsa_circ_0058092. (A) Predicted binding sites for miR-217 in hsa_circ_0058092. Mutated (Mut) version of hsa_circ_0058092 is also shown. (B) Relative luciferase activity was determined at 48 h following transfection with miR-217 mimic/NC or hsa_circ_0058092 wild-type/Mut in 293T cells. Data are presented as the means ± SD. ***P<0.001. (C) RT-qPCR detection of miR-217 expression in EPCs transfected with or without hsa_circ_0058092 overexpression vector and treated with or without HG. Data are presented as the means ± SD. ***P<0.001 vs. NC; $^{###}$P<0.001 vs. HG. (D) RT-qPCR detection of miR-217 expression following treatment with miR-217 inhibitor. Data are presented as the means ± SD. ***P<0.001 vs. NC; $^{###}$P<0.001 vs. HG. (E) CCK-8 assay for the proliferation of EPCs. Data are presented as the means ± SD. **P<0.01, ***P<0.001 vs. NC; $^{##}$P<0.01 vs. HG. (F and G) Transwell assays for the migration of EPCs. ***P<0.001 vs. control; $^{###}$P<0.001 vs. HG. Scale bar, 95 μm. (H and I) EPC tube formation capacity was measured (magnification, x200). Data are presented as the means ± SD. **P<0.01, ***P<0.001 vs. control; $^{###}$P<0.001 vs. HG. (J) Expression of oxidative stress proteins NOX1 and NOX4 was measured by western blot analysis. GAPDH served as an internal control. (K-M) Levels of inflammatory cytokines IL-1β, IL-6 and TNF-α were measured by ELISA. Data are presented as the means ± SD. ***P<0.001 vs. control; $^{###}$P<0.001 vs. HG. EPCs, endothelial progenitor cells; HG, high glucose.

bioinformatics analyses were performed to predict direct interactions between miR-217 and hsa_circ_0058092 (Fig. 3A). A luciferase reporter assay revealed that miR-217 inhibited luciferase activity in the cells transfected with the wild-type hsa_circ_0058092 luciferase reporter vector. Luciferase activity was not affected in the cells transfected with a mutated hsa_circ_0058092 luciferase reporter vector. This suggests that miR-217 is a target of hsa_circ_0058092 (Fig. 3B). RT-qPCR analysis revealed that HG conditions increased the expression of miR-217, while the overexpression of hsa_circ_0058092 suppressed the HG-induced expression of miR-217 (Fig. 3C). This further confirmed that miR-217 is a target of hsa_circ_0058092.

To determine whether miR-217 exerts a regulatory effect on EPCs under HG conditions, the EPCs were pre-treated with an miR-217 inhibitor. The results revealed that the HG-induced expression of miR-217 was suppressed in the cells that were pre-treated with the miR-217 inhibitor (Fig. 3D). The results of CCK-8 assay also revealed that HG suppressed EPC proliferation, while miR-217 inhibition partly restored the EPC proliferative capacity under HG conditions (Fig. 3E). Transwell migration experiments also demonstrated that the HG-mediated inhibition of EPC migration was restored by the downregulation of miR-217 (Fig. 3F and G). The EPC tube formation capacity was also decreased under HG conditions and was recovered by the downregulation of miR-217 (Fig. 3H and I). Western blot analysis also revealed that HG increased the expression of NOX4 and NOX1, while miR-217 inhibition prevented the increase in NOX1 and NOX4 protein expression (Fig. 3J). In addition, the HG-induced expression of TNF-α, IL-1β and IL-6 was suppressed by the downregulation of miR-217 (Fig. 3K-M). Taken together, these results

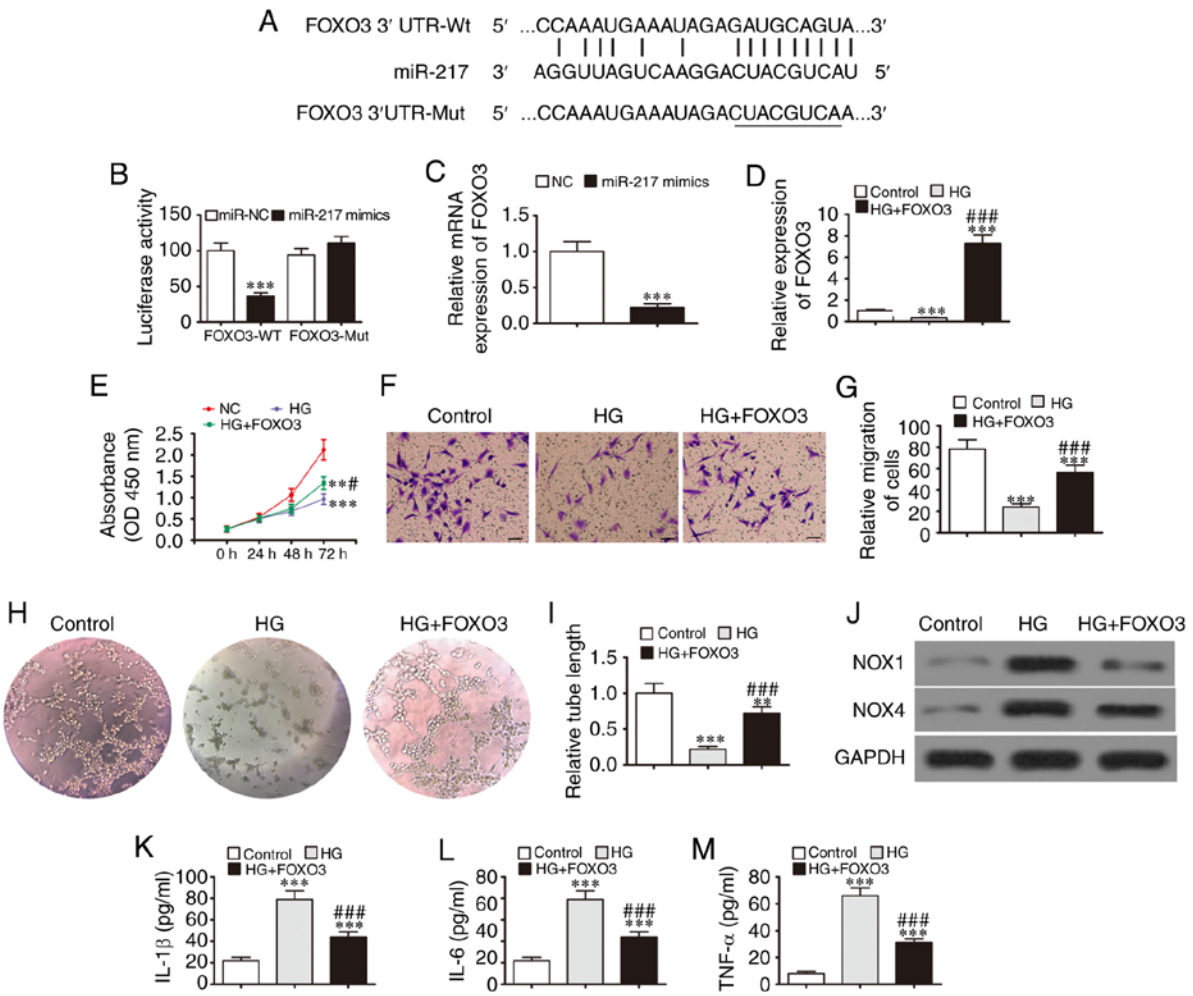

Figure 4. FOXO3 is a target of miR-217. (A) Predicted binding sites for miR-217 in FOXO3 3'UTR. Mutated (Mut) version of 3'UTR-FOXO3 is also shown. (B) Relative luciferase activities were determined at 48 h following transfection with miR-217 mimic/NC or 3'UTR-FOXO3 wild-type/Mut in 293T cells. Data are presented as the means ± SD. ***P<0.001. (C) RT-qPCR detection of FOXO3 expression in EPCs transfected with miR-217 mimic. Data are presented as the means ± SD. ***P<0.001 vs. NC. (D) RT-qPCR detection shows miR-217 and FOXO3 expression in EPCs following transfection with or without FOXO3 overexpression vector under HG conditions. Data are presented as the means ± SD. ***P<0.001 vs. control; $^{###}$P<0.001 vs. HG. (E) CCK-8 assay for the proliferation of EPCs. Data are presented as the means ± SD. **P<0.01, ***P<0.001 vs. control; $^{\#}$P<0.05 vs. HG. (F and G) Transwell experiments for the migration of EPCs. ***P<0.001 vs. control; $^{###}$P<0.001 vs. HG. Scale bar, 95 μm. (H and I) EPC tube formation capacity was measured (magnification, x200). Data are presented as the means ± SD. **P<0.01, ***P<0.001 vs. NC; $^{###}$P<0.001 vs. HG. (J) Expression of oxidative stress proteins NOX1 and NOX4 was measured by western blot analysis. GAPDH served as an internal control. (K-M) Levels of the inflammatory cytokines, IL-1β, IL-6 and TNF-α, were measured by ELISA. Data are presented as the means ± SD. ***P<0.001 vs. control. $^{###}$P<0.001 vs. HG. EPCs, endothelial progenitor cells; HG, high glucose.

demonstrate that miR-217 facilitates the damaging effects of HG on EPC proliferation, migration, tube formation and survival.

FOXO3 is a target of miR-217. Bioinformatics analysis also predicted that miR-217 directly interacts with the FOXO3 3'UTR (Fig. 4A). A luciferase reporter assay revealed that miR-217 inhibited luciferase activity in cells transfected with a wild-type FOXO3 luciferase reporter vector. However, the luciferase activity was not affected in cells transfected with a mutated FOXO3 luciferase reporter vector, suggesting that FOXO3 is a target of miR-217 (Fig. 4B). An RT-qPCR assay revealed that the overexpression of miR-217 suppressed FOXO3 expression (Fig. 4C), further confirming that FOXO3 is a target of miR-217.

To determine whether FOXO3 exerts a regulatory effect on EPC under HG conditions, a FOXO3 overexpression vector was constructed and transfected into EPCs prior to HG induction. The data verified that the HG conditions decreased FOXO3 expression, and this expression was recovered and upregulated following transfection with the FOXO3 overexpression vector (Fig. 4D). The results of CCK-8 revealed that FOXO3 overexpression restored the EPC proliferative capacity under HG conditions (Fig. 4E). Transwell migration assays also revealed that the inhibitory effects of HG on EPC migration were blocked by the overexpression of FOXO3 (Fig. 4F and G). The EPC tube formation capacity was also decreased under HG conditions and this decrease was blocked by the overexpression of FOXO3 (Fig. 4H and I). Western blot analysis revealed that NOX4 and NOX1 expression was increased under HG conditions, while FOXO3 overexpression prevented the increase in NOX4 and NOX1 protein expression (Fig. 4J). In addition, the HG-induced expression of the inflammatory cytokine, TNF-α, IL-1β and IL-6, was suppressed by the overexpression of FOXO3 (Fig. 4K-M). Taken together, these data indicate that the overexpression of FOXO3 exerted a protective effect

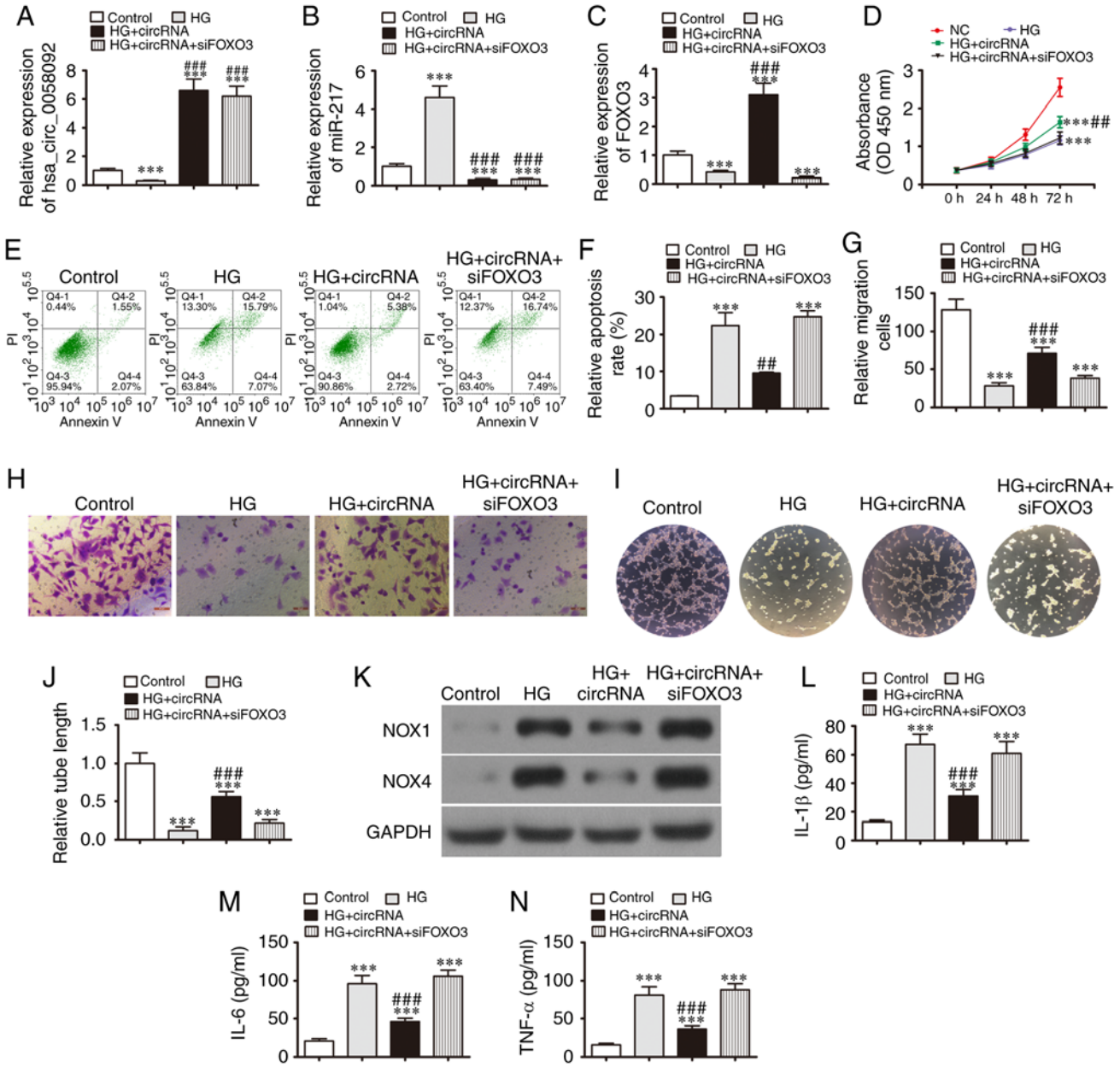

Figure 5. Overexpression of miR-217 or downregulation of FOXO3 reverses the protective effects of hsa_circ_0058092 on EPC proliferation, migration and angiogenic differentiation. (A-C) RT-qPCR detection for the expression of (A) hsa_circ_0058092, (B) miR-217 and (C) FOXO3 in EPCs. Data are presented as the means ± SD. ***P<0.001 vs. control; $^{###}$P<0.001 vs. HG. (D) CCK-8 assay for the proliferation of EPCs. Data are presented as the means ± SD. ***P<0.001 vs. control; $^{##}$P<0.01 vs. HG. (E and F) EPC apoptotic rate was determined by Annexin V/PI staining 24 h following induction with HG (30 mM). Data are presented as the means ± SD. ***P<0.001 vs. control; $^{##}$P<0.01 vs. HG. (G and H) Transwell assays for the migration of EPCs. Data are presented as the means ± SD. ***P<0.001 vs. control; $^{###}$P<0.001 vs. HG. Scale bar, 95 μm. (I and J) EPC tube formation capacity was measured (magnification, x200). Data are presented as the means ± SD. ***P<0.001 vs. control; $^{###}$P<0.001 vs. HG. (K) Expression of the oxidative stress proteins, NOX1 and NOX4, was measured by western blot analysis. GAPDH served as n internal control. (L-N) Levels of the inflammatory cytokines, IL-1β IL-6 and TNF-α, were measured by ELISA. Data are presented as the means ± SD. ***P<0.001 vs. control; $^{###}$P<0.001 vs. HG.

on EPC survival, proliferation, migration and tube formation under HG conditions.

Protective effects of hsa_circ_0058092 on EPC proliferation, migration and angiogenic differentiation are reversed by the overexpression of miR-217 or downregulation of FOXO3. The present study then aimed to identify an interactive association between hsa_circ_0058092, miR-217 and FOXO3 in relation to EPC proliferation, migration and angiogenic differentiation. The EPCs were transfected with an hsa_circ_0058092 overexpression vector or FOXO3 siRNA prior to induction with HG. The results of RT-qPCR demonstrated that induction with HG promoted the expression of miR-217, whereas it suppressed the expression of hsa_circ_0058092 and FOXO3. The overexpression of hsa_circ_0058092 downregulated miR-217 and upregulated FOXO3 expression. FOXO3 silencing had no effect on the expression of hsa_circ_0058092 or miR-217 (Fig. 5A-C). These results indicated that hsa_circ_0058092 regulated the expression of FOXO3 by miR-217 adsorption. The results of CCK-8 assay demonstrated that the overexpression of hsa_circ_0058092 restored the proliferative capacity of the EPCs under HG conditions, while FOXO3 silencing suppressed the

protective effects of hsa_circ_0058092 (Fig. 5D). EPC apoptosis was assessed by Annexin V/PI staining at 24 h following HG induction. The data revealed that the overexpression of hsa_circ_0058092 protected the EPCs against HG-induced apoptosis, while the silencing of FOXO3 again suppressed the protective effects of hsa_circ_0058092 (Fig. 5E and F). The results of Transwell migration assays also revealed that the overexpression of hsa_circ_0058092 protected against the HG-induced inhibition of EPC migration, while FOXO3 silencing suppressed the protective effects of hsa_circ_0058092 (Fig. 5G and H). The overexpression of hsa_circ_0058092 protected against the HG-induced impairment of EPC tube formation capacity. However, FOXO3 downregulation suppressed the protective effects of hsa_circ_0058092 on EPC tube formation (Fig. 5I and J). Western blot analysis also revealed that the overexpression of hsa_circ_0058092 prevented the HG-mediated induction of NOX4 and NOX1 proteins, while FOXO3 silencing suppressed the protective effects of hsa_circ_0058092 on oxidative stress in EPCs (Fig. 5K). Finally, the overexpression of hsa_circ_0058092 prevented the HG-induced increase in the levels of the inflammatory cytokines, TNF-α, IL-1β and IL-6, and the protective effects of hsa_circ_0058092 were attenuated following the FOXO3 of silencing under HG conditions (Fig. 5L-N). Taken together, these data suggest that hsa_circ_0058092 downregulates miR-217, which in turn upregulates FOXO3 expression and ultimately protects against HG-induced EPC damage.

Discussion

HG induces the impaired function of circulating progenitor cell populations (23,24). Although the precise underlying mechanisms remain unknown, the production of excessive ROS occurs due to the elevated levels of vascular NOX. Persistent HG can also induce the expression of inflammatory cytokines, which further damages EPCs (25,26). EPC injury suppresses cellular capacity for migration and angiogenic differentiation, which ultimately results in delayed wound healing (27,28). Therefore, in order to improve wound healing, it is necessary to identify the factors that regulate these microenvironments.

The present study observed a decreased expression of hsa_circ_0058092 under HG conditions. Previous research has indicated that certain circRNAs are aberrantly expressed in patients with T2DM and that these molecules may influence angiogenic mechanisms by regulating endothelial cell migration, proliferation and tube formation (29). The present study found that the upregulation of hsa_circ_0058092 protected against HG-induced damage to EPC proliferation, migration and tube formation.

It has been indicated that circRNAs function as miRNA sponges (30). The present study observed that miR-217 was a target of hsa_circ_0058092. It has been demonstrated that miR-217 serum levels are upregulated in patients with diabetic foot ulcers when compared to healthy controls (31). The suppression of miR-217 protects against HG-induced podocyte injury and insulin resistance by restoring phosphatase and tensin homologue-mediated autophagy pathways (32). The present study also found that the downregulation of miR-217 suppressed the HG-induced damage to EPCs by recovering cell survival, proliferation, migration and tube formation capacities. The luciferase reporter assay confirmed than an interactive association existed between hsa_circ_0058092 and miR-217.

Bioinformatics analysis also predicted that miR-217 interacts with FOXO3 3'UTR to suppress FOXO3 at the post-transcriptional level. It has been previously found that FOXO3 expression is reduced under HG conditions (33). The present study found that the overexpression of FOXO3 protected against HG-induced damage in EPC cell survival, proliferation, migration and tube formation capacity. Moreover, FOXO3 silencing suppressed the protective effects of hsa_circ_0058092 with respect to HG-induced damage to EPCs. FOXO proteins are transcription factors that participate in several cellular processes, such as immune cell homeostasis, cytokine production, cell proliferation and anti-oxidative stress mechanisms. The downregulation of FOXO3 inhibits cell proliferation, invasion and migration (34). FOXO3 is also critical for endothelial cell survival under HG conditions and has been implicated in the development of diabetes-induced retinal vascular endothelial cell injury (33). The present study observed that the downregulation of FOXO3 under HG conditions played an important role in the induction of EPC damage.

In conclusion, the present study observed that hsa_circ_0058092 expression was downregulated and that the decreased expression of this circRNA was associated with EPC damage under HG conditions. Although the complexity of the *in vivo* cellular crosstalk cannot be replicated in *in vitro* experiments, the data from the present study revealed that the overexpression of hsa_circ_0058092 protected against HG-induced damage to EPC angiogenesis and migration, and that these protective effects were regulated via the miR-217/FOXO3 signaling pathway. These results provide novel insight into the management and treatment of endothelial dysfunction in DM.

Acknowledgements

Not applicable.

Funding

No funding was received.

Availability of data and materials

All data generated or analyzed during this study are included in this published article or are available from the corresponding author on reasonable request.

Authors' contributions

JC, FZ, and WH performed research, processing of figures/images, providing materials and analyzed results. YW and ML designed the research and drafted the manuscript. All authors have read and approved the final manuscript.

Ethics approval and consent to participate

The present study was approved by the Ethics Committee of the Tenth People's Hospital of Tongji University after obtaining informed patient consent (SHDSYY-2019-3322).

Patient consent for publication

Not applicable.

Competing interests

The authors declare that they have no competing interests.

References

1. Barakat A, Nakao S, Zandi S, Sun D, Schmidt-Ullrich R, Hayes KC and Hafezi-Moghadam A: In contrast to Western diet, a plant-based, high-fat, low-sugar diet does not exacerbate retinal endothelial injury in streptozotocin-induced diabetes. FASEB J 33: 10327-10338, 2019.
2. Bin-Jaliah I, Hewett PW, Al-Hashem F, Haidara MA, Kader DHA, Morsy MD and Al-Ani B: Insulin protects against type 1 diabetes mellitus-induced aortopathy associated with the inhibition of biomarkers of vascular injury in rats. Arch Physiol Biochem: 1-7, Jun 28, 2019 (Epub ahead of print).
3. Zhang R, Liu J, Yu S, Sun D, Wang X, Fu J, Shen J and Xie Z: Osteoprotegerin (OPG) promotes recruitment of endothelial progenitor cells (EPCs) via CXCR4 signaling pathway to improve bone defect repair. Med Sci Monit 25: 5572-5579, 2019.
4. Dvorin EL, Wylie-Sears J, Kaushal S, Martin DP and Bischoff J: Quantitative evaluation of endothelial progenitors and cardiac valve endothelial cells: Proliferation and differentiation on poly-glycolic acid/poly-4-hydroxybutyrate scaffold in response to vascular endothelial growth factor and transforming growth factor beta1. Tissue Eng 9: 487-493, 2003.
5. Rethineswaran VK, Kim YJ, Jang WB, Ji ST, Kang S, Kim DY, Park JH, Van LTH, Giang LTT, Ha JS, *et al*: Enzyme-aided extraction of fucoidan by AMG augments the functionality of EPCs through regulation of the AKT/Rheb signaling pathway. Mar Drugs 17: 392, 2019.
6. Jin H, Zhang Z, Wang C, Tang Q, Wang J, Bai X, Wang Q, Nisar M, Tian N, Wang Q, *et al*: Melatonin protects endothelial progenitor cells against AGE-induced apoptosis via autophagy flux stimulation and promotes wound healing in diabetic mice. Exp Mol Med 50: 1-15, 2018.
7. Gao J, Zhao G, Li W, Zhang J, Che Y, Song M, Gao S, Zeng B and Wang Y: MiR-155 targets PTCH1 to mediate endothelial progenitor cell dysfunction caused by high glucose. Exp Cell Res 366: 55-62, 2018.
8. Rosso A, Balsamo A, Gambino R, Dentelli P, Falcioni R, Cassader M, Pegoraro L, Pagano G and Brizzi MF: p53 Mediates the accelerated onset of senescence of endothelial progenitor cells in diabetes. J Biol Chem 281: 4339-4347, 2006.
9. Kadam S, Kanitkar M, Dixit K, Deshpande R, Seshadri V and Kale V: Curcumin reverses diabetes-induced endothelial progenitor cell dysfunction by enhancing MnSOD expression and activity in vitro and in vivo. J Tissue Eng Regen Med 12: 1594-1607, 2018.
10. Sosale B, Chandrashekara S, Aravind SR, Renuka P and Anupama KR: Influence of cytokine status on insulin resistance and circulating endothelial progenitor cells in type 2 diabetes mellitus. Cytokine 99: 179-185, 2017.
11. Cortes-Lopez M and Miura P: Emerging functions of circular RNAs. Yale J Biol Med 89: 527-537, 2016.
12. Huang G, Li S, Yang N, Zou Y, Zheng D and Xiao T: Recent progress in circular RNAs in human cancers. Cancer Lett 404: 8-18, 2017.
13. Wu H, Wu S, Zhu Y, Ye M, Shen J, Liu Y, Zhang Y and Bu S: Hsa_circRNA_0054633 is highly expressed in gestational diabetes mellitus and closely related to glycosylation index. Clin Epigenetics 11: 22, 2019.
14. Zhao Z, Li X, Jian D, Hao P, Rao L and Li M: Hsa_circ_0054633 in peripheral blood can be used as a diagnostic biomarker of pre-diabetes and type 2 diabetes mellitus. Acta Diabetol 54: 237-245, 2017.
15. Xu H, Guo S, Li W and Yu P: The circular RNA Cdr1as, via miR-7 and its targets, regulates insulin transcription and secretion in islet cells. Sci Rep 5: 12453, 2015.
16. Fang Y, Wang X, Li W, Han J, Jin J, Su F, Zhang J, Huang W, Xiao F, Pan Q and Zou L: Screening of circular RNAs and validation of circANKRD36 associated with inflammation in patients with type 2 diabetes mellitus. Int J Mol Med 4: 1865-1874, 2018.
17. Wang H, She G, Zhou W, Liu K, Miao J and Yu B: Expression profile of circular RNAs in placentas of women with gestational diabetes mellitus. Endocr J 66: 431-441, 2019.
18. Li WD, Zhou DM, Sun LL, Xiao L, Liu Z, Zhou M, Wang WB and Li XQ: LncRNA WTAPP1 promotes migration and angiogenesis of endothelial progenitor cells via MMP1 through MicroRNA 3120 and Akt/PI3K/autophagy pathways. Stem Cells 36: 1863-1874, 2018.
19. Wu Z, Huang W, Wang X, Wang T, Chen Y, Chen B, Liu R, Bai P and Xing J: Circular RNA CEP128 acts as a sponge of miR-145-5p in promoting the bladder cancer progression via regulating SOX11. Mol Med 24: 40, 2018.
20. Livak KJ and Schmittgen TD: Analysis of relative gene expression data using real-time quantitative PCR and the 2(-Delta Delta C(T)) method. Methods 25: 402-408, 2001.
21. Wu H, Chen Z, Chen JZ, Xie J and Xu B: Resveratrol improves tube formation in AGE-induced late endothelial progenitor cells by suppressing syndecan-4 shedding. Oxid Med Cell Longev 2018: 9045976, 2018.
22. Shen S, Wu Y, Chen J, Xie Z, Huang K, Wang G, Yang Y, Ni W, Chen Z, Shi P, *et al*: CircSERPINE2 protects against osteoarthritis by targeting miR-1271 and ETS-related gene. Ann Rheum Dis 78: 826-836, 2019.
23. Loomans CJ, de Koning EJ, Staal FJ, Rookmaaker MB, Verseyden C, de Boer HC, Verhaar MC, Braam B, Rabelink TJ and van Zonneveld AJ: Endothelial progenitor cell dysfunction: A novel concept in the pathogenesis of vascular complications of type 1 diabetes. Diabetes 53: 195-199, 2004.
24. Kränkel N, Adams V, Linke A, Gielen S, Erbs S, Lenk K, Schuler G and Hambrecht R: Hyperglycemia reduces survival and impairs function of circulating blood-derived progenitor cells. Arterioscler Thromb Vasc Biol 25: 698-703, 2005.
25. Lontchi-Yimagou E, Sobngwi E, Matsha TE and Kengne AP: Diabetes mellitus and inflammation. Curr Diab Rep 13: 435-444, 2013.
26. Karam BS, Chavez-Moreno A, Koh W, Akar JG and Akar FG: Oxidative stress and inflammation as central mediators of atrial fibrillation in obesity and diabetes. Cardiovasc Diabetol 16: 120, 2017.
27. Boniakowski AE, Kimball AS, Jacobs BN, Kunkel SL and Gallagher KA: Macrophage-mediated inflammation in normal and diabetic wound healing. J Immunol 199: 17-24, 2017.
28. Salazar JJ, Ennis WJ and Koh TJ: Diabetes medications: Impact on inflammation and wound healing. J Diabetes Complications 30: 746-752, 2016.
29. Zhang SJ, Chen X, Li CP, Li XM, Liu C, Liu BH, Shan K, Jiang Q, Zhao C and Yan B: Identification and characterization of circular RNAs as a new class of putative biomarkers in diabetes retinopathy. Invest Ophthalmol Vis Sci 58: 6500-6509, 2017.
30. Memczak S, Jens M, Elefsinioti A, Torti F, Krueger J, Rybak A, Maier L, Mackowiak SD, Gregersen LH, Munschauer M, *et al*: Circular RNAs are a large class of animal RNAs with regulatory potency. Nature 495: 333-338, 2013.
31. Lin CJ, Lan YM, Ou MQ, Ji LQ and Lin SD: Expression of miR-217 and HIF-1α/VEGF pathway in patients with diabetic foot ulcer and its effect on angiogenesis of diabetic foot ulcer rats. J Endocrinol Invest 42: 1307-1317, 2019.
32. Sun J, Li ZP, Zhang RQ and Zhang HM: Repression of miR-217 protects against high glucose-induced podocyte injury and insulin resistance by restoring PTEN-mediated autophagy pathway. Biochem Biophys Res Commun 483: 318-324, 2017.
33. Chen Y, Wang Y, Jiang Y, Zhang X and Sheng M: High-glucose treatment regulates biological functions of human umbilical vein endothelial cells via sirt1/FOXO3 pathway. Ann Transl Med 7: 199, 2019.
34. Li W and Jiang H: Up-regulation of miR-498 inhibits cell proliferation, invasion and migration of hepatocellular carcinoma by targeting FOXO3. Clin Res Hepatol Gastroenterol 44: 29-37, 2020.